

Fermi arcs and hidden zeros of the Green function in the pseudogap state

Tudor D. Stanescu and Gabriel Kotliar

Center for Materials Theory, Department of Physics and Astronomy, Rutgers University, Piscataway, New Jersey 08854-8019, USA

(Received 5 June 2006; published 25 September 2006)

We investigate the low-energy properties of a correlated metal in the proximity of a Mott insulator within the Hubbard model in two dimensions. We introduce a version of the cellular dynamical mean-field theory using cumulants as the basic irreducible objects. The cumulants are used for reconstructing the lattice quantities from their cluster counterparts. The zero-temperature one-particle Green function is characterized by the appearance of lines of zeros, in addition to a Fermi surface which changes topology as a function of doping. We show that these features are intimately connected to the opening of a pseudogap in the one-particle spectrum and provide a simple picture for the appearance of Fermi arcs.

DOI: [10.1103/PhysRevB.74.125110](https://doi.org/10.1103/PhysRevB.74.125110)

PACS number(s): 71.10.Fd, 71.27.+a

I. INTRODUCTION

The origin of the pseudogap persists as one of the leading unresolved problems in the physics of the copper-oxide high-temperature superconductors.¹ Since a large part of the physics of these systems arises from short-range correlations, cluster extensions of single-site dynamical mean-field theory² (DMFT) are ideally suited for this problem. In fact, using such methodologies, several groups have found³ that a pseudogap, as evidenced by a suppression of the density of states at the Fermi level, appears near the doped Mott insulator as described by the Hubbard model. This effect is caused solely by short-range correlations and no long-range order or preformed pairs need to be invoked. In the present work we present an extension of the cluster methodology that allows us to identify the emergence of lines of zeros of the Green function at zero energy (i.e., the Luttinger surface) in addition to the quasiparticle poles (i.e., the Fermi surface), in the proximity of the Mott transition. These results are similar to those found in quasi-one-dimensional systems by Essler and Tselik.⁶ The appearance and the evolution of a pseudogap in the particle spectral function is governed by the topology of these lines. At small hole doping, the Fermi surface, i.e., the line of poles, is a hole pocket, having a Luttinger surface in close proximity. The quasiparticle weights along a portion of the Fermi contour are suppressed by the proximity of the zero line, generating the Fermi arc behavior of the spectral function which was identified experimentally.¹²

The zeros of the Green function correspond to a diverging self-energy along certain lines in the Brillouin zone at zero temperature. The finite temperature precursors of these divergences are present in cluster DMFT calculations for both the one-dimensional (1D) and two-dimensional (2D) Hubbard models, using either momentum space¹⁵ or real space¹⁴ cluster schemes. A self-energy that is large or diverging in momentum space will be long range in real space. This situation seems to contradict the assumptions that are at the heart of DMFT, namely, that the physics of the system is driven by short-range correlations that can be captured by a local or a short-range self-energy. In this paper we address this issue by developing a different cluster DMFT scheme based on cumulant as the basic irreducible quantity, instead of the self-

energy. Unlike the self-energy, the cumulant remains short ranged and therefore, it is better suited to describe the strong correlations that characterize the system in or near the Mott insulating phase.

The paper is organized as follows: In Sec. II we first introduce the cumulant cluster DMFT approach which represents a strong-coupling generalization of the cellular DMFT technique, together with an alternative procedure in which the self-consistent bath function is constructed using *lattice* quantities instead of *cluster* quantities. We use this alternative procedure as a consistency check to ensure that the results are free from any possible artifacts coming from the superlattice construction. In the second part of Sec. II we benchmark our procedure by calculating the kinetic energy of the 1D Hubbard model and comparing the results with those obtained using the Bethe ansatz. We also consider the half-filled 2D Hubbard model as an example of a system characterized by diverging self-energies and show how the problem can be solved within the cumulant approach. In Sec. III we analyze the low-energy physics of a strongly correlated metal using our cumulant technique. We show how a pseudogap develops at the Fermi level as a result of the presence of a line of zeros in the zero frequency Green function. We define the Fermi line as the location in k space of the poles of the Green function and show that the arclike appearance of the spectral function results from the interplay between the Fermi line and the line of zeros. Our conclusions are presented in Sec. IV.

II. STRONG COUPLING CLUSTER DYNAMICAL MEAN-FIELD THEORY

A. The formalism

We formulate a new cluster approach based on a resummation of a strong coupling expansion around the atomic limit, which generalizes the cellular dynamical mean-field theory (CDMFT) scheme.⁵ We use the notations of Ref. 4, for a general lattice Hamiltonian,

$$H = H_0 + H_1 = \sum_i \sum_{\alpha} \lambda_{\alpha} X_i^{\alpha\alpha} + \sum_{i \neq j} \sum_{\alpha, \beta, \alpha', \beta'} E_{ij}^{\alpha\beta\alpha'\beta'} X_i^{\alpha\beta} X_j^{\alpha'\beta'}, \quad (1)$$

where the local, H_0 , and the nonlocal, H_1 , terms are expressed in terms of Hubbard operators $X_i^{\alpha\beta}$. Here $\alpha, \beta, \alpha', \beta'$,

and β' represent single-site states. All the on-site contributions, such as, for example, the Hubbard U interaction, are included in λ_{α} , while the nonlocal coupling constants $E_{ij}^{\alpha\beta\alpha'\beta'}$ can be understood as generalized hopping matrix elements and may include hopping terms (t_{ij}), spin-spin interactions (J_{ij}), or nonlocal Coulomb interactions (V_{ij}).

A cluster DMFT scheme⁵ maps the lattice model onto an effective impurity problem on a real-space cluster \mathcal{C} , defined by the statistical operator

$$e^{-\beta H_{c0}} \hat{T} \exp \left\{ - \int_0^\beta d\tau \int_0^\beta d\tau' X_a^\mu(\tau) \times [\Delta_{ab}^{\mu\nu}(\tau - \tau') + \delta_{\tau, \tau'} E_{ab}^{\mu\nu}] X_b^\nu(\tau') + \int_0^\beta d\tau h_a^\mu(\tau) X_a^\mu(\tau) \right\}, \quad (2)$$

where $H_{c0} = \sum_{a \in \mathcal{C}} \sum_{\alpha} \lambda_{\alpha} X_a^{\alpha\alpha}$ is the local cluster Hamiltonian, \hat{T} represents the imaginary time-ordering operator, and we used the notation $(\alpha\beta) = \mu$. The hybridization $\Delta_{ab}^{\mu\nu}$ and the effective magnetic field h_a^μ are the Weiss fields describing the effects of the rest of the system on the cluster.

A cluster DMFT approach to a lattice problem consists of two elements: (1) a recipe for expressing the Weiss fields in terms of cluster quantities, i.e., a self-consistency condition, and (2) a recipe for determining lattice quantities from the relevant cluster counterparts, i.e., a periodization procedure. To carry out the first step, we follow the CDMFT approach and construct a superlattice by translating a cluster \mathcal{C} so as to cover the original lattice and treat the cells as “single” sites with internal degrees of freedom. The self-consistency equation for $\Delta_{ab}^{\mu\nu}$ is determined by the condition that the Green function for the Hubbard operators be the same for a cell and for the impurity cluster

$$\sum_{\kappa \in RBZ} [\hat{\mathbf{M}}_c^{-1} - \hat{\mathbf{E}}_\kappa]^{-1} = [\hat{\mathbf{M}}_c^{-1} - \hat{\Delta} - \hat{\mathbf{E}}]^{-1}, \quad (3)$$

where we used the tensor notation $\hat{\mathbf{A}} = A_{ab}^{\mu\nu}$ with a and b labeling the sites inside the cluster of size N_c , and $\mu = (\alpha, \beta)$, $\nu = (\alpha', \beta')$. In Eq. (3) M_c is the irreducible two-point cumulant of the cluster defined as the sum of all two-point diagrams generated by the strong coupling expansion of Eq. (2) that are irreducible with respect to E and Δ ; E represents the coupling constant matrix and the κ summation is performed over the reduced Brillouin zone associated with a superlattice with cells of size N_c . The Weiss field h_a^μ is determined by

$$\sum_{i \in \mathcal{C}} \sum_{\nu} E_{ai}^{\mu\nu} \langle X_i^\nu \rangle = h_a^\mu + \sum_{b \in \mathcal{C}} \sum_{\nu} \Delta_{ab}^{\mu\nu}(0) \langle X_b^\nu \rangle, \quad (4)$$

where the hybridization is evaluated at zero frequency. Within our approach, the cluster problem defined by Eq. (2) has to be solved self-consistently together with Eqs. (3) and (4). Notice that only cluster quantities, in particular the irreducible cumulant M_c , enter the self-consistency loop.

The impurity model delivers cluster quantities and, to make connection with the original lattice problem, we need to infer from them estimates for the lattice Green function. A

natural way to produce these estimates is by considering the superlattice construction described before and averaging the relevant quantities, which we denote below by W , to restore periodicity, namely,

$$W(i-j) \approx \frac{1}{N_s} \sum_{k, k+i-j} W_{k, k+i-j}^{SL}, \quad (5)$$

where W and W^{SL} are the lattice and superlattice quantities, respectively, and N_s represents the total number of sites. We stress that Eq. (5) represents a superlattice average, not a cluster average. In particular, if W is the irreducible cumulant, all the contributions with k and $k+i-j$ belonging to different cells are zero by construction. One possibility⁷ is to periodize the Green function

$$\mathbf{G}(\mathbf{k}, \omega) = \frac{1}{N_{c,a,b \in \mathcal{C}}} \sum [\hat{\mathbf{M}}_c^{-1} - \hat{\mathbf{E}}_{\mathbf{k}}]_{ab}^{-1} e^{i\mathbf{k}(\mathbf{r}_a - \mathbf{r}_b)}, \quad (6)$$

$\hat{\mathbf{E}}_{\mathbf{k}}$ being the Fourier transform of the “hopping” on the superlattice, and N_c the number of sites in a cell. A second possibility, suggested by the strong coupling approach investigated in this paper, is to first periodize the irreducible cumulant and then use it to reconstruct the lattice Green function $\hat{\mathbf{G}}(\mathbf{k}, \omega) = [\hat{\mathbf{M}}^{-1}(\mathbf{k}, \omega) - \hat{\mathbf{E}}_{\mathbf{k}}]^{-1}$. For example, within a four-site approximation (plaquette) we obtain after performing the average (5) and then taking the Fourier transform,

$$\mathbf{M}(\mathbf{k}, \omega) = \mathbf{M}_0(\omega) + \mathbf{M}_1(\omega)\alpha(\mathbf{k}) + \mathbf{M}_2(\omega)\beta(\mathbf{k}), \quad (7)$$

where $\alpha(\mathbf{k}) = \cos(k_x) + \cos(k_y)$, $\beta(\mathbf{k}) = \cos(k_x)\cos(k_y)$, and $M_{p=\{0,1,2\}}$ represents the on-site, nearest-neighbor, and next-nearest-neighbor cluster cumulant, respectively.

To test the dependence of the approach on the superlattice construction, we also introduce an alternative self-consistency condition that involves the periodized lattice quantities, instead of the cluster quantities that appear in Eq. (3), in the spirit of periodized cellular dynamical mean-field theory (PCDMFT)⁸ but satisfying an explicit cavity construction. We define the hybridization function Δ as the sum of all the contributions to the cluster irreducible cumulant coming from outside the cluster and being connected to bare cumulants inside the cluster by two hopping lines, namely,

$$\Delta_{ab}(i\omega_n) = \sum_{A,B} \mathbf{E}_{aA} \mathbf{K}_{AB}(i\omega_n) \mathbf{E}_{Bb}, \quad (8)$$

where we used the matrix notation $\mathbf{W}_{ab} = W_{ab}^{\mu\nu}$ and the matrix multiplication over μ and ν is implied. In Eq. (8), $\mathbf{K}_{AB}(i\omega_n)$ represents the cavity propagator, i.e., a Green function which does not contain contributions arising from irreducible cumulants having at least one-site index inside a certain cluster \mathcal{C} of size N_c . We assume that \mathbf{M}_{ij} has a finite range $|\mathbf{r}_i - \mathbf{r}_j| < R$, so that the terms that we subtract from the lattice cumulants to construct the cavity form a matrix \mathbf{M}^* which is nonzero only inside an extended cluster \mathcal{C}_{ext} containing sites that can be coupled with the original cluster by a nonzero cumulant. Explicitly, $\mathbf{M}_{ij}^* = \mathbf{M}_{ij}$ if at least one of the indexes belongs to the cluster \mathcal{C} and zero otherwise, which ensures that \mathbf{M}_{ij}^* is contained in \mathcal{C}_{ext} . The propagator $\mathbf{K}_{AB}(i\omega_n)$ is a generalization of the cavity function² and we are interested to

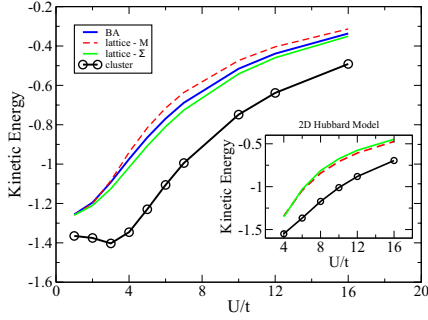


FIG. 1. (Color online) Kinetic energy of the half-filled 1D Hubbard model as a function of the on-site interaction U at zero temperature using: the Bethe ansatz (blue/dark gray line), the cluster Green function (black line with circles), and the lattice Green function obtained by periodizing the self-energy (green/light gray line) and the irreducible cumulant (dashed red line). The inset shows the kinetic energy for the 2D case (same color code). The Green function periodization scheme (not shown) produces results that are almost identical with those given by the cumulant scheme. The results were obtained using CDMFT with an exact diagonalization (ED) impurity solver.

express it in terms of the lattice Green function for sites (A, B) that can be connected with the cluster \mathcal{C} via a hopping line. We assume that $(A, B) \in \mathcal{C}_{ext}$, i.e., the hopping has the same range as \mathbf{M}_{ij} or smaller. For the extended cluster the cavity propagator can be written as

$$\hat{\mathbf{K}} = \hat{\mathbf{G}} - \hat{\mathbf{H}}\hat{\mathbf{M}}^*[\hat{\mathbf{I}} + \hat{\mathcal{E}}\hat{\mathbf{M}}^*]^{-1}\hat{\mathbf{H}}, \quad (9)$$

where all the matrices \mathbf{W}_{AB} are defined on the extended cluster, $A, B \in \mathcal{C}_{ext}$, \mathbf{G} is the lattice Green function corresponding to the irreducible lattice cumulant \mathbf{M} , $\mathbf{H}_{AB} = (\mathbf{G}\mathbf{M}^{-1})_{AB}$, and $\mathcal{E}_{AB} = (\mathbf{E}\mathbf{H}^{-1})_{AB}$. The lattice Green function can be expressed directly in terms of cluster cumulants using Eq. (7) as

$$\hat{\mathbf{G}}^{-1}(\mathbf{k}, \omega) = [\mathbf{M}_0(\omega) + \mathbf{M}_1(\omega)\alpha(\mathbf{k}) + \mathbf{M}_2(\omega)\beta(\mathbf{k})]^{-1} - \hat{\mathbf{E}}_{\mathbf{k}}. \quad (10)$$

We note that Eq. (8) together with Eqs. (9) and (10) can be viewed as an independent cluster scheme with variations that can be generated using different choices for the cavity matrix \mathbf{M}^* . This alternative cluster method allows us to check that our results are self-consistent by reintroducing the lattice cumulant into the DMFT equations. This is important since previous results of a straightforward strong-coupling expansion were shown to disappear in a more sophisticated DMFT treatment.⁹

B. A benchmark for the reconstruction procedure and the problem of diverging self-energies

We benchmark our approach, as in Ref. 10, by computing the kinetic energy of the half-filled 1D Hubbard model which is given exactly from the Bethe ansatz. We also make a comparison with the alternative periodization procedures involving the Green function and the self-energy. Shown in Fig. 1 is the kinetic energy of the half-filled 1D Hubbard model. The exact result from the Bethe ansatz (continuous blue/dark

gray line) is used as a benchmark. We notice that the values of the kinetic energy given by the cluster Green function (black line and circles) are significantly different from the exact result, while the curves obtained using the lattice Green function, extracted using various procedures, cluster around the Bethe ansatz line. We notice that the results obtained by periodizing the Green function (not shown) and those obtained by periodizing the cumulant (dashed red line) are remarkably similar, especially in the strong coupling regime. We observe a very similar behavior in the 2D case shown in the inset. We conclude that within CDMFT and other related cluster schemes, when applied to small clusters, observables should be always extracted from the physical lattice quantities and *not* from their cluster counterparts. Because in our generalized strong-coupling construction of the cluster approximations hopping is treated on equal footing with other nonlocal contributions to the Hamiltonian, such as spin-spin interaction, the conclusions derived from the calculation of the kinetic energy extend to all nonlocal physical quantities, for example, to the spin-spin correlation function. In contrast with nonlocal quantities, the local physical quantities are well approximated by their cluster values which have to be preserved by the reconstruction schemes. For a homogeneous cluster (as, for example, the link or the plaquette), periodizing the Green function automatically satisfies this condition for all one-particle quantities as, by construction, $G_{ii}^{latt} = G_{aa}^c$. The cumulant periodization scheme also generates a local Green function in good agreement with G^c . However, the self-energy scheme fails at half filling and for small-doping values as it generates spurious states in the gap.

To support our statements we consider as an example the half-filled 2D Hubbard model with $U=8t$ and solve the quantum problem within a 2×2 cluster approximation (plaquette) using CDMFT and an exact diagonalization solver. The results for the irreducible cluster quantities, i.e., for the cumulant and the self-energy, as functions of the Matsubara frequency are shown in Fig. 2. The local nature of the cumulant is revealed by the comparison between the local cumulant M_{11} , and the next-nearest-neighbor component M_{13} . Due to the particle-hole symmetry at half filling, these components are purely imaginary, in contrast with the link cumulant M_{12} which is real. We notice that $M_{11} \gg M_{13}$ for all frequencies. In contrast, the corresponding components of the self-energy, Σ_{11} and Σ_{13} , become comparable at low frequencies, as shown in the inset of Fig. 2. This is a consequence of the nonlocal nature of the self-energy. Moreover, Σ_{11} and Σ_{13} diverge at zero frequency. This divergence is the cluster signature of divergence along the $(\pi, 0) \rightarrow (0, \pi)$ line in momentum space that characterizes the half-filled 2D Hubbard model with $t'=0$. One can show that, within the 2×2 (plaquette) approximation, the $(\pi, 0)$ and $(0, \pi)$ points of the Brillouin zone are controlled by the double-degenerate diagonal cluster self-energy $\Sigma_A = \Sigma_{11} - \Sigma_{13}$. In addition, the points (π, π) and $(0, 0)$ are controlled by the other two diagonal self-energies, $\Sigma_B = \Sigma_{11} - 2\Sigma_{12} + \Sigma_{13}$ and $\Sigma_C = \Sigma_{11} + 2\Sigma_{12} + \Sigma_{13}$, respectively. In our case Σ_A diverges at zero frequency, while Σ_B and Σ_C remain finite.

Finally, using the same example of the half-filled 2D Hubbard model, let us compare the cumulant and self-energy

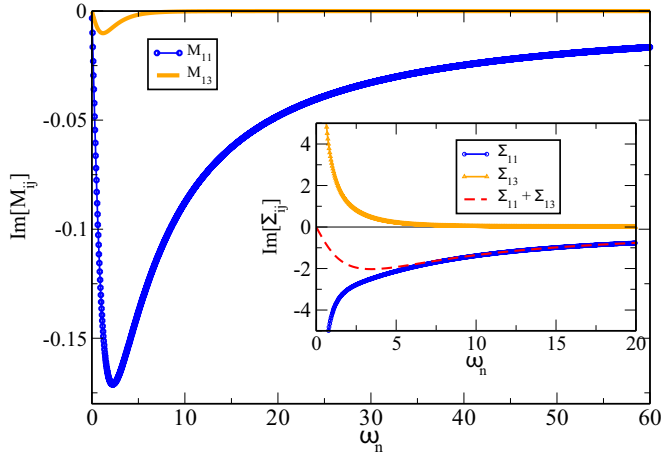


FIG. 2. (Color online) Cluster cumulant as a function of the imaginary frequency for the half-filled 2D Hubbard model with $U = 8t$. We compare the on-site cumulant M_{11} (blue/dark gray) with the next-nearest-neighbor cumulant M_{13} (orange/light gray), as both components are purely imaginary. The nearest-neighbor cumulant M_{12} (not shown) is real. Notice that $\text{Im}[M_{13}] \ll \text{Im}[M_{11}]$ for all frequencies, as a result of the local nature of the cumulant. The inset shows the imaginary components of the cluster self-energy, Σ_{11} (blue/dark gray) and Σ_{13} (orange/light gray). Notice that (i) both components diverge as $\omega_n \rightarrow 0$, and (ii) the two components become comparable at small energies, as proved by the vanishing of the sum $\Sigma_{11} + \Sigma_{13}$ (dashed red line). This behavior is a result of the nonlocal nature of the self-energy.

reconstruction schemes. The results for the on-site lattice Green function are shown in Fig. 3 and compared with the cluster local Green function. The agreement between the lattice local Green function obtained using the cumulant reconstruction scheme and the cluster G_{11} is striking. In contrast, the self-energy periodization scheme fails. This failure is a direct consequence of the nonlocal nature of the self-energy.

We have constructed a cluster DMFT scheme that uses cumulants as basic irreducible quantities. This approach addresses the serious problem of the nonlocality of the self-energy in the vicinity of a Mott insulating phase by identifying a local irreducible quantity, the cumulant. Next, we study some of the implications of this new perspective on the low-energy physics of a correlated metal.

III. PSEUDOGAPS, FERMI ARCS, AND THE ZEROS OF THE GREEN FUNCTION

As an application of our method to a strongly correlated metal, we study the weakly doped 2D Hubbard model using a four-site cluster approximation. In general, the lattice Green function can be written as

$$G(\mathbf{k}, \omega) = \frac{1}{\omega - r(\mathbf{k}, \omega) - i\eta(\mathbf{k}, \omega)}, \quad (11)$$

where $\eta(\mathbf{k}, \omega)$ represents the imaginary part of the self-energy and $r(\mathbf{k}, \omega) = \epsilon(\mathbf{k}) - \mu + \text{Re}\Sigma(\mathbf{k}, \omega)$ is the energy. In the self-energy periodization scheme doping values, $\Sigma(\mathbf{k}, \omega)$ is a linear combination of the lattice self-energies given by

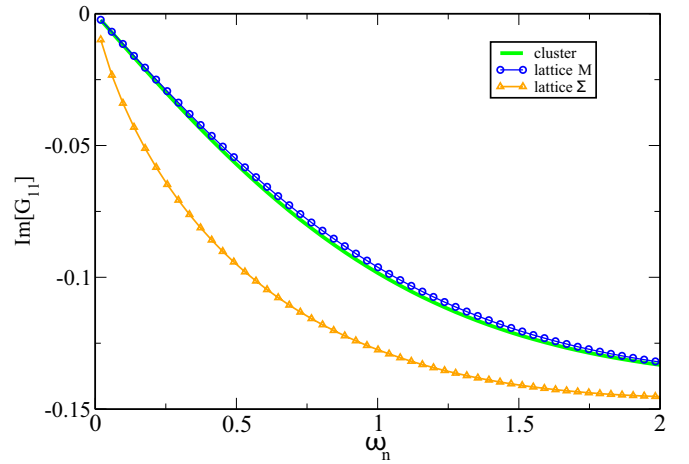


FIG. 3. (Color online) Comparison of the local cluster Green function (green line) with the lattice local Green function calculated using the cumulant periodization scheme (blue circles) and the self-energy periodization scheme (orange triangles). The good agreement between the cluster G_{11} and the lattice Green function obtained using cumulants is a result of the local nature of this irreducible quantity. In contrast, the self-energy is nonlocal and the reconstruction scheme based on Σ fails. The results are for a 2D half-filled Hubbard model with $U = 8t$ and were obtained using a four-site cluster CDMFT with an ED impurity solver.

$$\Sigma(\mathbf{k}, \omega) = \Sigma_0(\omega) + \Sigma_1(\omega)\alpha(\mathbf{k}) + \Sigma_2(\omega)\beta(\mathbf{k}). \quad (12)$$

In the cumulant reconstruction scheme, which describes better the system near the Mott transition, the lattice self-energy is given by a highly nonlinear relation

$$\Sigma(\mathbf{k}, \omega) = \omega - \mu - \left[\frac{\frac{1}{2}(1-\beta)}{\omega + \mu - \Sigma_A} + \frac{\frac{1}{4}(1-\alpha+\beta)}{\omega + \mu - \Sigma_B} + \frac{\frac{1}{4}(1+\alpha+\beta)}{\omega + \mu - \Sigma_C} \right]^{-1}, \quad (13)$$

where $\alpha(\mathbf{k})$ and $\beta(\mathbf{k})$ were defined above, and the diagonal cluster self-energies are $\Sigma_A = \Sigma_0 - \Sigma_2$ and $\Sigma_{B(C)} = \Sigma_0 \mp 2\Sigma_1 + \Sigma_2$. Using exact diagonalization as an impurity solver¹¹ one finds that at zero temperature the imaginary parts of the cluster self-energies go to zero at zero frequency. For the real parts, on the other hand, we distinguish two regimes. At large dopings the diagonal cluster self-energies are dominated by the local component Σ_0 and Eq. (13) reduces in the first approximation to Eq. (12). In this regime the physics is almost local with small corrections due to short-range correlations. All the periodization schemes converge and the single-site DMFT represents a good first-order approximation. In contrast, close to the Mott transition the short-range correlations become important and the off-diagonal components of the cluster self-energy become comparable with Σ_0 . As a consequence, at zero frequency the denominators in Eq. (13) may acquire opposite signs generating a divergence in the lattice self-energy. This pole of $\Sigma(\mathbf{k}, \omega=0)$, or equivalently of $r(\mathbf{k})$, gives rise to a zero of the lattice Green function. We show in Fig. 4 the renormalized energy $r(\mathbf{k})$ and the spectral

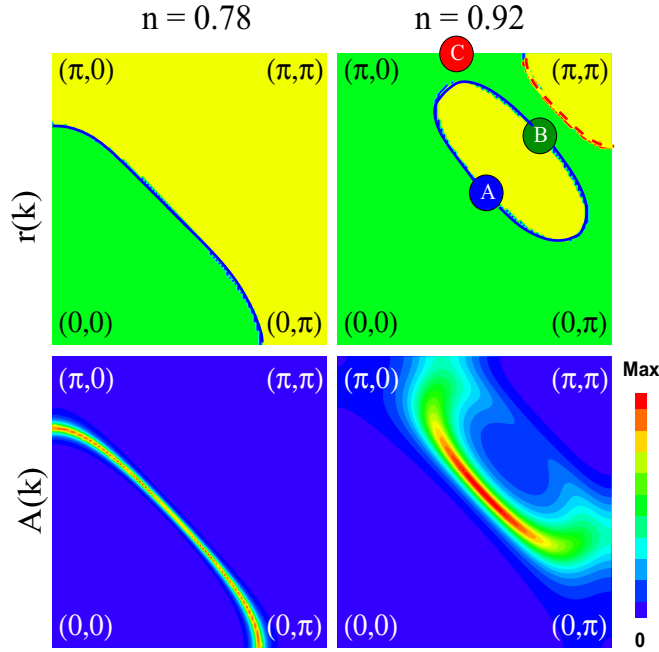


FIG. 4. (Color online) Renormalized energy $r(\mathbf{k})$ (upper panels) and spectral function $A(\mathbf{k})$ (lower panels) for the 2D Hubbard model with $U=8t$ and $T=0$. The color code for the upper panels is green/gray ($r < 0$), blue/dark gray line ($r = 0$), yellow/light gray ($r > 0$), red dashed line ($r \rightarrow \infty$). The frequency dependence of the spectral function for the points marked by A, B, and C is shown in Fig. 5.

function $A(\mathbf{k}, \omega=0) = -1/\pi \text{Im}G(\mathbf{k}, 0)$ for a 2D Hubbard model with $U=8t$ at zero temperature for two values of doping. For $n=0.78$ (left panels) we have a large electron-type Fermi surface [blue/dark gray line in the $r(\mathbf{k})$ panel] separating the occupied region of the Brillouin zone (green/gray), defined by $r(\mathbf{k}) < 0$ from the unoccupied region (yellow/light gray) defined by $r(\mathbf{k}) > 0$. The Fermi surface can be also traced in the $A(\mathbf{k})$ panel as the maximum of the spectral function. On the other hand, for $n=0.92$ a qualitatively different picture emerges. The Fermi surface (blue/dark gray line) is now represented by a hole pocket and, in addition, we have a line of zeros of the Green function (red dashed line) close to the (π, π) region of the Brillouin zone. Furthermore, there is no one-to-one correspondence between the Fermi surface and the maximum of the spectral function. This behavior has two origins, (1) the proximity of a zero line suppresses the weight of the quasiparticle on the far side of the pocket, and (2) for k points corresponding to $r(\mathbf{k}) \neq 0$ the quasiparticles are pushed away from $\omega=0$ and a pseudogap opens at the Fermi level. We show this explicitly in Fig. 5 by comparing the low frequency dependence of the spectral function in three different points of the Brillouin zone, marked by A, B and C in Fig. 4. Notice the suppression of the zero-frequency peak at point B and the frequency shift $\delta = -0.05t$ of the peak at point C. The cumulant approach provides a simple interpretation of this effect, observed in photoemission experiments,¹² in terms of the emergence of infinite self-energy lines or equivalently Luttinger lines (lines of zeros of the Green function).

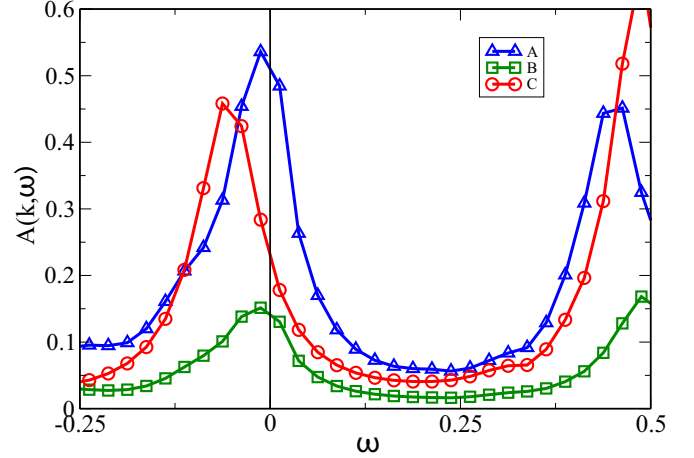


FIG. 5. (Color online) Frequency dependence of the spectral function for three points in the Brillouin zone marked by A, B, and C in Fig. 4. Point A (blue line with triangles) is on the Fermi surface, close to $(\pi/2, \pi/2)$; point B (green squares) is on the “dark side” of the Fermi surface, in the vicinity of the zero line; and point C (red circles) is in the pseudogap region on the line and corresponding to the maxima of the spectral function (see Fig. 4). Notice that the leading edge gap is quantitatively much smaller than the distance between the peaks at positive and negative energy.

IV. CONCLUSIONS

In conclusion, our strong coupling CDMFT study of the Hubbard model shows that the lightly doped system is characterized by a small, closed Fermi line that appears in the zero-frequency spectral function as an arc due to the presence of a line of zeros of the Green function near the “dark side” of the Fermi surface. These lines of poles of the self-energy appear near the Mott insulator and have the important consequence of violating the Luttinger relation between the number of particles and the volume of the Fermi surface as determined by the poles of the Green function.¹³ The vanishing of both the real and imaginary parts of the Green function at specific locations in the Brillouin zone is an appealing scenario that is consistent with the growth of the real and imaginary parts of the self-energy as the temperature is reduced. This is the hallmark of the Mott transition in CDMFT,¹¹ and should be contrasted with the weak coupling scenario where the real part of the self-energy is regular, and only the imaginary part exhibits singularities. The divergence of the self-energy in certain points of the Brillouin zone is observed in cluster DMFT calculation, using both real space¹⁴ (CDMFT) and momentum space¹⁵ cluster schemes. This behavior seems at odds with the very spirit of DMFT and shows that the self-energy is not the appropriate quantity to describe Mott physics governed by short-range correlations. We argue that the irreducible quantity that should be used to describe this physics is the two-point cumulant. In particular for the Hubbard model, a precursor of the self-energy divergence can be observed even for values of the on-site interaction smaller than the bandwidth.¹⁵ A critical reevaluation of the data for this regime from the cumulant perspective would be extremely useful.

Notice that while the zeros of the Green function only appear in the limit of zero temperature, they have clear finite temperature signatures in the pseudogap, as seen in the leading-edge study of photoemission experiments. We identify this pseudogap as the small negative shift of the spectral weight in points of the Brillouin zone that are not on the Fermi line (for example, point *C* in Fig. 4). This is a much smaller energy scale than the larger gap between the peaks above and below the Fermi level (see Fig. 5), which has been stressed in earlier cluster DMFT studies. Remarkably, the lines of poles of the self-energy appear first far from the Fermi surface. This is a strong coupling instability which has no weak coupling precursors on the Fermi surface. Our results raise an interesting question. If the evolution in Fig. 4 from large to small doping is continuous, it has to go through

a critical point where the topology of the Fermi surface (and perhaps that of the lines where the self-energy is infinite) changes. This topological change and its possible connection to an underlying critical point at finite doping in the cuprate phase diagram deserves further investigation.

ACKNOWLEDGMENTS

This research was supported by the NSF under Grant No. DMFT-0528969 and by the Rutgers University Center for Materials Theory. Many useful discussions with M. Civelli, B. Kyung, A. M. Tremblay, M. Capone, O. Parcollet, and A. Tsvelik are gratefully acknowledged. Special thanks to K. Haule and M. Civelli for allowing the use of their ED and NCA programs.

-
- ¹T. Timusk and B. Statt, Rep. Prog. Phys. **62**, 61 (1999).
²A. Georges, G. Kotliar, W. Krauth, and M. J. Rozenberg, Rev. Mod. Phys. **68**, 13 (1996).
³T. Maier, M. Jarrel, T. Pruschke, and J. Keller, Eur. Phys. J. B **13**, 613 (2000); M. Jarrel, T. Maier, M. H. Hettler, and A. N. Tahvildar-Zadeh, Europhys. Lett. **56**, 563 (2001); T. D. Stanescu and P. Phillips, Phys. Rev. Lett. **91**, 017002 (2003); D. Sénéchal and A.-M. S. Tremblay, *ibid.* **92**, 126401 (2004); B. Kyung, S. S. Kancharla, D. Sénéchal, A.-M. S. Tremblay, M. Civelli and G. Kotliar, Phys. Rev. B **73**, 165114 (2006).
⁴T. D. Stanescu and G. Kotliar, Phys. Rev. B **70**, 205112 (2004).
⁵G. Kotliar, S. Y. Savrasov, G. Palsson, and G. Biroli, Phys. Rev. Lett. **87**, 186401 (2001).
⁶F. H. L. Essler and A. M. Tsvelik, Phys. Rev. B **65**, 115117 (2002).
⁷D. Sénéchal, D. Perez, and M. Pioro-Ladrière, Phys. Rev. Lett. **84**, 522 (2000).
⁸G. Biroli, O. Parcollet, and G. Kotliar, Phys. Rev. B **69**, 205108 (2004).
⁹S. Biermann, A. Georges, A. Lichtenstein, and T. Giamarchi, Phys. Rev. Lett. **87**, 276405 (2001).
¹⁰M. Capone, M. Civelli, S. S. Kancharla, C. Castellani, and G. Kotliar, Phys. Rev. B **69**, 195105 (2004).
¹¹M. Civelli, M. Capone, S. S. Kancharla, O. Parcollet, and G. Kotliar, Phys. Rev. Lett. **95**, 106402 (2005).
¹²D. S. Marshall, D. S. Dessau, A. G. Loeser, C.-H. Park, A. Y. Matsuura, J. N. Eckstein, I. Bozovic, P. Fournier, A. Kapitulnik, W. E. Spicer, and Z.-X. Shen, Phys. Rev. Lett. **76**, 4841 (1996); M. R. Norman, H. Ding, M. Randeria, J. C. Campuzano, T. Yokoya, T. Takeuchi, T. Takahashi, T. Mochiku, K. Kadowaki, P. Guptasarma, and D. G. Hinks, Nature (London) **392**, 157 (1998); A. Damascelli, Z. X. Shen, and Z. Hussain, Rev. Mod. Phys. **75**, 473 (2003).
¹³A. A. Abrikosov, L. P. Gorkov, and I. E. Dyaloshinskii, *Methods of Quantum Field Theory in Statistical Physics* (Pergamon, Elmsford, New York, 1965). When singularities are present in the self-energy the integral $\int G \frac{\partial \Sigma}{\partial \omega} = I$ is not necessarily zero. See, for example, A. Georges, O. Parcollet, and S. Sachdev, Phys. Rev. B **63**, 134406 (2001). Hence the number of particles is equal to the area contained by the surface of zeros and the area contained by the surface of poles of the Green function plus the anomaly *I*.
¹⁴B. Kyung, G. Kotliar, and A.-M. S. Tremblay, Phys. Rev. B **73**, 205106 (2006).
¹⁵Th. A. Maier, Th. Pruschke, and M. Jarrell, Phys. Rev. B **66**, 075102 (2002).